Int J Clin Exp Pathol 2014;7(5):2044-2055
www.ijcep.com /ISSN:1936-2625/IJCEP0000011

Original Article

Nogo-C contributes to HCC tumorigenesis via suppressing cell growth and its interactome analysis with comparative proteomics research

Xing Liu[1,2*], Shu-Jian Cui[3*], Shi-Jun Zhu[4], De-Chun Geng[4], Long Yu[1]

[1]State Key Laboratory of Genetic Engineering, Fudan University, Shanghai, China; [2]National Engineering Center for Biochip at Shanghai, Shanghai, China; [3]College of Bioscience and Biotechnology, Key Laboratory of Crop Genetics and Physiology of Jiangsu Province, Yangzhou University, Yangzhou, China; [4]Department of Orthopaedic Surgery, The First Affiliated Hospital of Soochow University, Suzhou, China. [*]Equal contributors.

Received February 17, 2014; Accepted March 4, 2014; Epub April 15, 2014; Published May 1, 2014

Abstract: Objects: Neurite outgrowth inhibitor proteins (Nogos) comprise a family of three major members and are characterized by a conserved RHD domain. Among all the members, Nogo-B was identified to be significantly elevated and to play an important role in liver cirrhosis while Nogo-C was the shortest one and received little attention. The aim of this study is to investigate the relevance and mechanism of Nogo-C involved in Hepatocellular carcinoma (HCC). Methods: The expression of Nogo-C in paired HCC specimens was measured with quantitative RT-PCR. The function of Nogo-C over expressing in SMMC-7721 and WRL-68 HCC cell lines were estimated through cell proliferation assay and colony formation assay. A proteome-wide identification of Nogo-C-binding proteins was performed using affinity purification combined with a highly sensitive mass spectrometric technique. The protein interactions were confirmed using co-IP and immunofluorescence confocal assays. Results: Compared with the neighboring pathologically normal tissues, the expression of Nogo-C mRNA was extremely down-regulated in HCC specimens and was significantly related to greater tumor size and worse prognosis. Overexpression of Nogo-C in HCC cell lines resulted in an inhibition of cell growth. A total of 73 proteins were detected and considered in association with Nogo-C, among which B-raf and Nogo-B were validated. Conclusion: We identify Nogo-C as a tumor suppressor gene in HCC and B-raf as a novel interacting protein. These findings provide new directions for the mechanism research of Nogo family.

Keywords: Nogo-C, HCC, tumor suppressor gene, comparative proteomics, interactome, B-raf

Introduction

Reticulon (RTN) 4 is one member of the RTN protein family characterized by a homologous carboxy terminal tail containing an endoplasmic reticulum (ER) targeting motif. RTN4 has three major splice forms termed as neurite outgrowth inhibitor protein (Nogo)-A, -B, and -C, which only differ in their amino terminal sequence. Among them, Nogo-C bears the simplest structure of a unique eleven-amino-acid N-terminal tail and a reticulon homology domain (RHD), comparing with other two transcripts [1]. The three Nogo family members have a broad tissue expression pattern and multiple functions over them. Nogo-A expresses mainly in nervous tissues and behaves as a neurite outgrowth inhibitor [2]. Nogo-B is found in many tissues and regulates vascular remodeling in pathological vascular conditions caused by ischemia, atherosclerosis, and other insults [3-8]. Compared with the two well defined members, research on Nogo-C remains limited. Previous work identified that exogenous expression of Nogo-C in Schwann cells of transgenic mice induced a delayed axonal regeneration while similar expression in SMMC-7721 cells resulted in apoptosis via JNK-c-Jun dependent pathway accompanied with p53 activation [9, 10], indicating its proapoptotic role under certain circumstances. However, given the high expression in skeletal muscle and nervous system, it seems that Nogo-C has ubiquitous roles other than participating in apoptosis [7, 11].

Recent studies have shown diversified expression levels of Nogo family proteins in different tumors. The elevated expression of Nogo-A was

detected correlated with the malignancy grading in oligodendroglial tumors, although its significance as a diagnostic marker was still argumentative [12-14]. It is also noteworthy that Nogo-B highly expresses in cervical cancer and induces cancer metastasis through Fibulin-5 [15]. However, current knowledge of expression and function of Nogo-C, as well as its possible mechanism in hepatocellular carcinoma (HCC) is still limited.

The co-IP protein identification technique is a new interaction detection experimental procedure based on the development of ultra-sensitive mass spectrometric techniques and it provides an important method for protein function exploring since it is crucial for all biological processes [16]. To unravel the mechanisms of Nogo-A and Nogo-B in regulating cell growth and migration, several in vitro approaches have been applied to identify Nogo protein complexes, including yeast two-hybrid interaction mating and AP-Nogo binding assay specifically searching for membrane proteins, in which the placental alkaline phosphatase (AP) is used as the affinity tag. Bcl-2, Bcl-xL, NIMP, membrane protein NgR and NgBR are identified as Nogo interaction proteins [17-19]. Yet, such large scale screening has not been done to Nogo-C.

In this study, we reported the down-regulated expression of Nogo-C and its correlations with clinic pathological features in HCC for the first time. Down-regulated expression was appeared in nearly 70% HCC specimens compared with the counterpart normal tissues, and tended to be correlated with greater tumor size and worse prognosis. In HCC cell lines, over-expression of Nogo-C resulted in lower tumor cell growth and colony formation. These results implicated the function of Nogo-C in inhibiting tumorigenesis. In addition, a comprehensively profile of Nogo-C interacting proteins were identified based on the proteomic research, among which Nogo-B and B-raf were confirmed to bind with Nogo-C. The evaluation of the data will allow us to better understand the function and mechanism of Nogo-C in inhibiting tumorigenesis.

Materials and methods

Cell lines and cell culture

In this study, liver tumor-derived cell lines SMMC-7721 and WRL-68 were used. Both cell lines were maintained in DMEM culture medium supplemented with 10% FBS in 5% CO_2 at 37°C.

Human tissue samples

Surgical specimens were obtained from Zhongshan Hospital (Shanghai, China), approved by the Clinical Research Ethics Committee of Zhongshan Hospital of Fudan University. The tumor tissues and the neighboring pathologically nontumorous liver tissues were immediately frozen in liquid nitrogen after surgery and then stored at -80°C for further analysis.

Reverse transcription polymerase chain reaction and real time polymerase chain reaction (RT-PCR)

Total RNA was extracted from tissues using Trizol reagent (Invitrogen) and 1 ug of RNA were applied for reverse transcription (TAKARA). Real-time PCR analysis was conducted SYBR Green Supermix kit (Takara) with the ABI7300 detection system. Properly diluted cDNA was used in a 20 μl RT-PCR reaction in triplicate for each gene. Cycle parameters were 95°C for 30 s hot start and 40 cycles of 95°C for 5 s and 60°C for 30 s.

Primers for Nogo-C were forward, 5'-TGTCTCAGGGAGTAGGTTTGTG-3', and reverse, 5'-TCCAGTACAGGAGGTCAACAA-3'. Primers for β-actin were forward, 5'-AATCGTGCGTGACATTAAGGAG-3', and reverse, 5'-ACTGTGTTGGCGTACAGGTCTT-3'.

Cell proliferation and colony formation assay

SMMC-7721 and WRL-68 cell lines were transfection with either Nogo-C-pcDNA3.1 or empty pcDNA3.1 plasmids, using lipofectamine 2000 reagent (Invitrogen). For cell proliferation assay, all cells were plated at a density of 2,000 cells per well in 96-well plates. During a 5-day culture period, cells were subjected to cck-8 (Dojindo Laboratories, Tokyo) every day. The absorbance of each well (n=6) was measured at 1 h after incubation by a microtiter reader (Bio-Tek) at 450 nm. For colony formation assay, transfected hepatoma cells were plated at a density of 5×10^4 per well in 6-well plates. G418 was added into the medium 24 h later. Colonies were identified by crystal violet staining after about 10 to 14 days of culture.

SDS-PAGE and in-gel digestion

The protein mixtures affinity-purified with anti-Myc antibody were separated by SDS-PAGE. After SDS-PAGE, each gel lane was equally cut into 5 pieces, 1.5 mm in width. The proteins within gel slices were treated with DTT and

iodoacetamide followed by in-gel digestion with trypsin.

Mass spectrometry (MS) analysis

The peptide mixtures of each piece were separation by RP chromatography (75 μm × 200 mm C18 column) and the peptides were eluted into a SYNAPT mass spectrometer coupled with a Nano LOCKSpray at a flow rate of 200 nL/min. NanoUPLC was used to deliver mobile phases A (0.1% formic acid in water) and B (0.1% formic acid in ACN) at a linear gradient from 5% B to 50% B within 60 min, along with a gradient from 50% B to 90% B within 30 min and a hold at 90% B for 5 min.

Spectra were acquired in high-definition MSE-mode switching every 1.2 seconds between low collision energy of 4 eV and high collision energy ramping from 15 eV to 40 eV. The acquired spectra were further processed with ProteinLynx Global Server (PLGS version 2.2.6, Waters, Milford, MA, USA) to reconstruct MS/MS spectra by combining all masses with identical retention times. The mass accuracy of the mass spectrometer was calibrated by the peak of m/z of 785.8426 Da [M+2H]2+ which was generated by glu-fibrinopeptide (GFP), when analyzed off-line at a concentration of 400 fmol/μl and a flow rate of 100 nl/min.

Mass data interpretation

The MS/MS spectra were searched against the human international protein index protein database (IPI ID: 2.66) downloaded from ftp://ftp.ebi.ac.uk/pub/databases/IPI/current/ [20]. The min fragment ion matches per peptide was set at three while the min fragment ion matches per protein was set at seven. The Min Peptide Matches Per Protein was configured to one. Two missed cleavage sites were allowed. Variable modifications of oxidation (M) and carbamidomethyl (C) were permitted. The false positive rate was fixed at 4%.

Coimmunoprecipitation (Co-IP) assay

Co-IP assay was taken to validate the proteins identified by MS. Plasmids encoding the identified candidate proteins and the bait Nogo-C were transfected into SMMC-7721 cells for 36 h before the cells were lysed using 1 × CLB. For co-IP, 10 μl protein A/G-Sepharose beads pre-absorbed with appropriate antibodies were utilized to isolate the immunocomplexes. The isolated beads were washed twice with CLB and twice with RIPA buffer (0.15 mM NaCl/0.05 mM Tris-HCl, pH 7.2/1% Triton X-100/1% sodium deoxycholate/0.1% SDS) [21]. Immunoblot (IB) analysis was conducted to probe the resolved complexes with indicated antibodies. Monoclonal anti-c-Myc antibody (clone 9E10; Chemicon) and monoclonal anti-HA antibody (clone 12CA5; Roche) were used for isolation and detection of the tagged Nogo-B, Nogo-C and B-Raf.

Immunofluorescence microscopy

Transfected SMMC-7721 cells were fixed with 4% paraformaldehyde for 15 min at room temperature, permeabilized with 0.1% Triton X-100. After blocking in phosphate-buffered saline (PBS) containing 5% BSA for 1 h, cells were immunostained with primary anti-Myc antibody (9E10) overnight at 4°C, followed by incubation with Cy3-conjugated anti-mouse immunoglobulin G antibody (Biological Detection Systems) at room temperature for 1 hours. To visualize nuclei, cells were incubated in 100 μg/ml 4,6-diamidino-2-phenylindole (DAPI) in PBS for 10 minutes. Coverslips were mounted and observed under Zeiss confocal microscope.

Bioinformatic and statistic data analyses

The Gene Ontology (GO) is the current standard for annotating gene products and proteins. The identified candidate proteins were annotated to the terms of molecular function and cellular component based on GO under standard procedure using Blast2Go [22] (http://www.blast2go.org/).

Non parametric test was used to determine the Spearman correlation between the Nogo-C expression level and the clinial characteristics (PRISM software version 5.0, GraphPad, San Diego, CA). A two-tailed Student's t test was used to evaluate the significance between grouped data. $P<0.05$ was considered statistically significant.

Result

Nogo-C was frequently down-regulated in HCC

We first assessed Nogo-C expression pattern in several normal human tissues using semi-quantitative PCR. Nogo-C was relatively abundant in the brain, heart, kidney and liver tis-

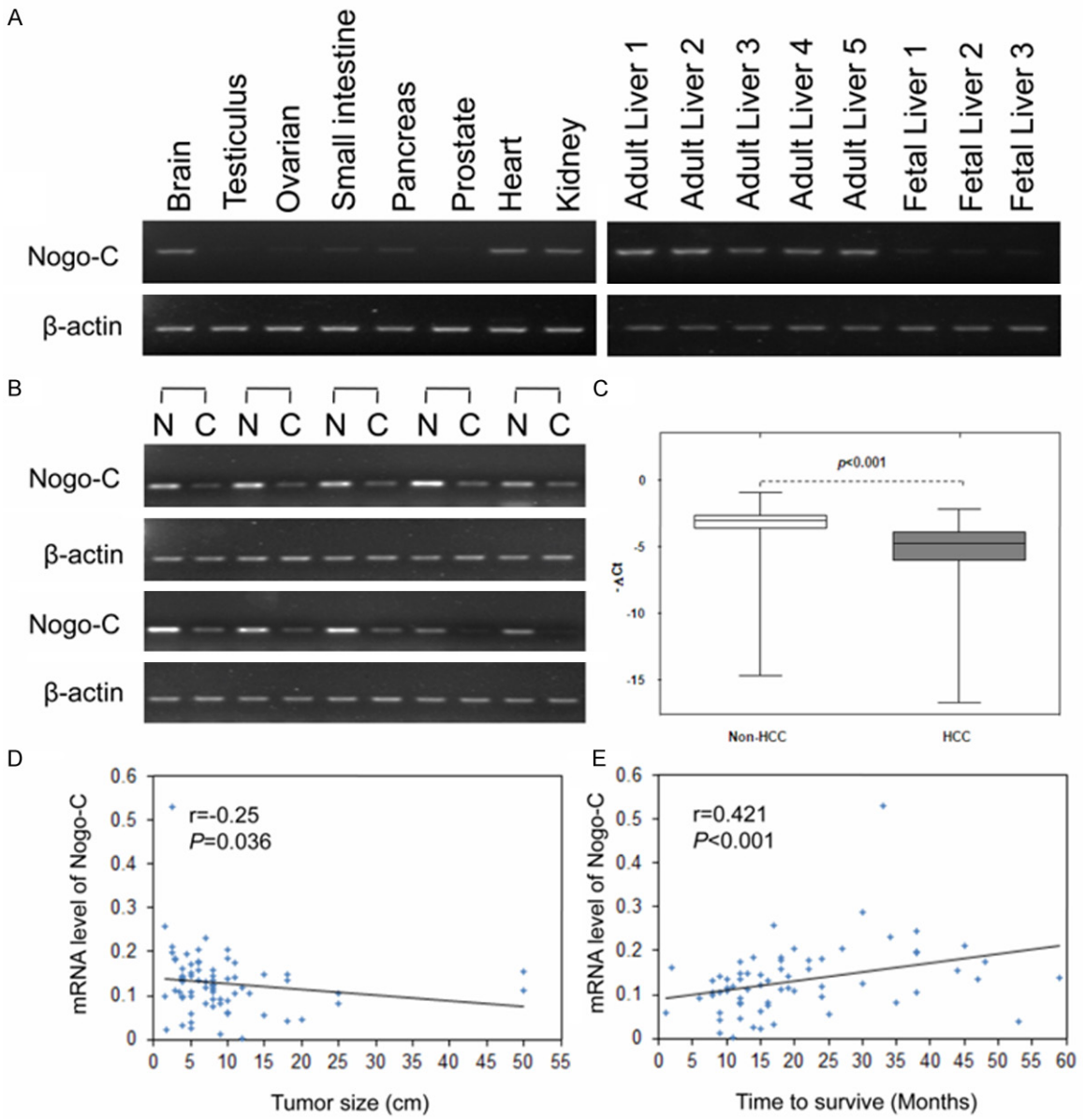

Figure 1. Down-regulated expression of Nogo-C in human hepatocellular carcinomas (HCC). (A) Semi-quantitative PCR analysis of Nogo-C expression in 9 human adult tissues and fatal liver. Expression of the human β-actin served as a loading control. (B) Nogo-C mRNA levels were analyzed in 6 paired HCCs with their corresponding non-cancerous specimens by semi-quantitative PCR. (C) Nogo-C mRNA expression levels in 76 paired HCC specimens with their corresponding neighboring nontumorous specimens measured by RT-PCR. (D and E) The Spearman correlation between tumor size (D) or between patient's living time and Nogo-C mRNA expression level in HCC specimens (E).

sues, with very low levels in fetal liver and other tissues (**Figure 1A**). In 10 pairs of HCC specimens with the matched non-tumor tissue counterparts, Nogo-C expression was extremely down-regulated (**Figure 1B**). To further explore the clinicopathological correlation of Nogo-C down-regulation in HCC tissues, the quantitative reverse transcriptase PCR assay was conducted to evaluate Nogo-C expression in other 76 HCC specimens. The result showed that the mRNA levels encoding Nogo-C was down-regulated (expression was decreased more than twofold) in 50 (65.8%) of 76 HCC specimens (**Figure 1C**). The expression level of Nogo-C in these HCC specimen appeared to be negatively correlated with HCC tumor size (r=-0.25, P=0.036) (**Figure 1D**). Patients with HCC with lower Nogo-C level had a shorter survival times

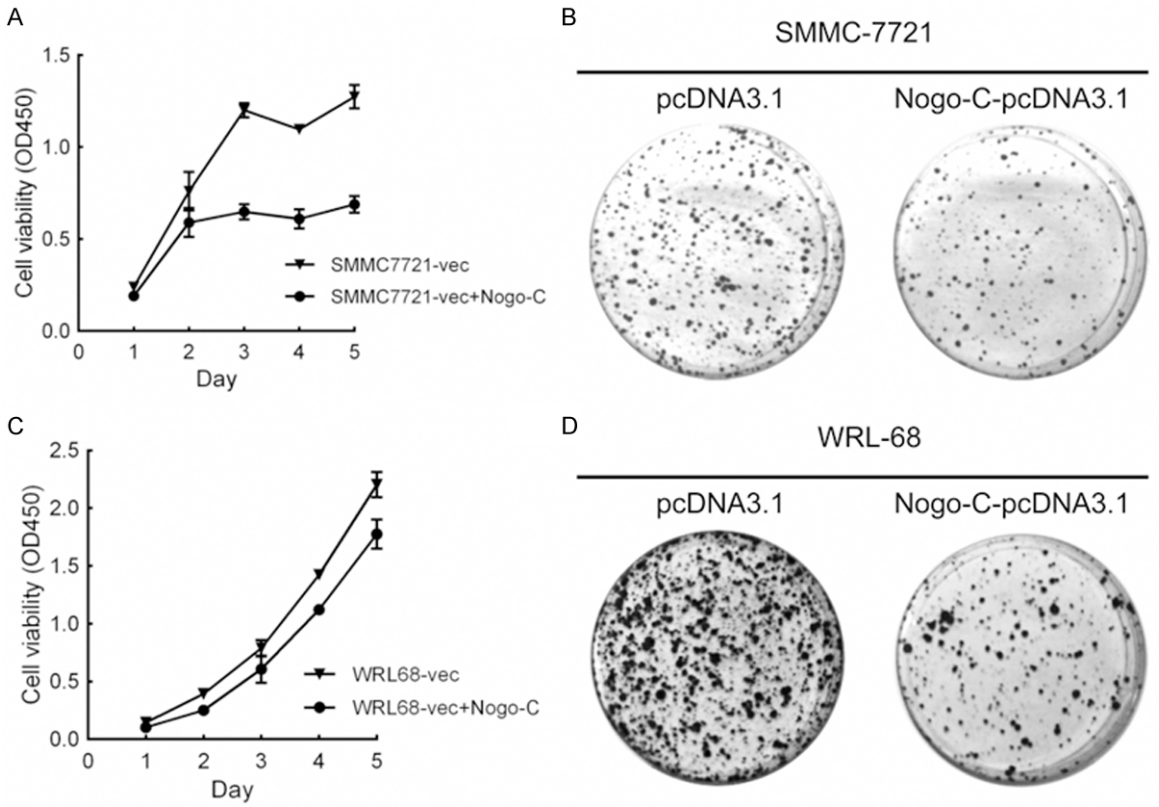

Figure 2. Overexpression of Nogo-C suppressed growth of HCC cell lines. (A and B) Exogenous Nogo-C was expressed in SMMC-7721 (A) and WRL-68 (B) cells transfected with the pcDNA3.1 vector. Empty vector were used as a control. The growth of these cells was analyzed using cck-8 kit. (C and D) Representative images of colony formation assay in SMMC-7721 (C) and WRL-68 (D).

than patients with HCC expressing high levels of Nogo-C ($r=0.421$, $P<0.001$, **Figure 1E**).

Nogo-C suppressed HCC cell growth

To evaluate whether Nogo-C function as a tumor suppressor gene in HCC cells, we further observed the effect of Nogo-C expression on cell proliferation and colony formation. SMMC-7721 and WRL-68 cells were transiently transfected with Nogo-C-pcDNA3.1 and control vector. Cell growth and colony formation of these cells were suppressed by Nogo-C overexpression (**Figure 2**).

Interactome analysis of Nogo-C

To identify Nogo-C interacting proteins, a proteomic analysis was carried out. The scheme of the strategy was shown in **Figure 3A**. Plasmids consisting of Nogo-C and the empty pCMV vectors were transfected into SMMC-7721 cells in parallel and the cell lysates were acquired separately. The transfection efficiency of the plasmids in both samples was evaluated using western blot (**Figure 3B**). Immunoprecipitations were done to both Nogo-C sample and pCMV sample using anti-Myc antibody. A combined one-dimensional PAGE with LC/MS/MS strategy was used to identify compartments of protein complexes. The vast majority of the sequence-matched spectra were of good quality and all the identified peptides were above the threshold score for identity with a confidence level of >95%. We assigned 2,261 distinct peptides with significant probability scores into 325 unique proteins in all, including 165 proteins identified in the Nogo-C sample and 160 proteins in the pCMV sample. All proteins were identified based on the presence of at least 2 peptide fragments. Ninety-one proteins identified in both samples and 69 proteins identified in the pCMV sample were excluded as non-specific binding proteins. Apart from the identified core protein Nogo-C, 73 proteins specifically detected in the Nogo-C sample were recognized as potential Nogo-C interacting pro-

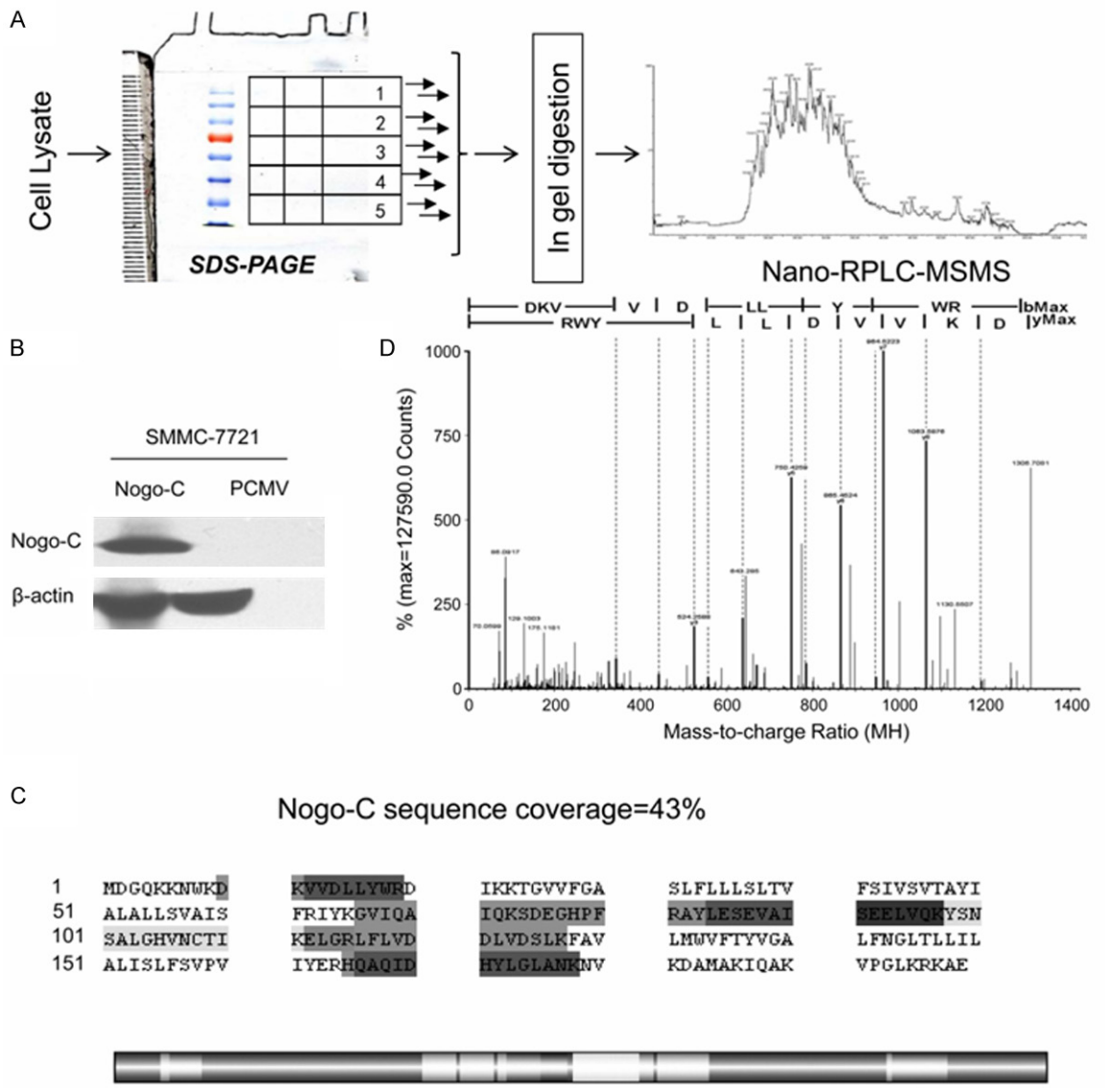

Figure 3. Proteomic analysis of Nogo-C binding proteins. A: The schematic flow chart of the MS-based proteomic analysis of the protein complexes. B: Ectogenous Myc-Nogo-C plasmids and the pCMV plasmids were transfected separately into SMMC-7721 cells. The presence or absence of Nogo-C on Western blots was revealed by probing with an anti-Myc antibody. β-actin was used as the loading control. C: Sequence coverage of Nogo-C (43%) from the 5 identified peptides (emphasized in gray) from the experiment. The distribution of the identified peptides of Nogo-C was shown in the strip chart in highlight. The dark gray section represented the overlapped sequences from identified proteins. D: One representative illustration of a MS/MS specific peptide of Nogo-C.

teins. Their information, including accession number (IPI#), protein name, molecular weight, number of detected peptides, PLGS score, PI (PH) and their molecular functions, were summarized in **Table 1**. It ought to be emphasized that the bait protein Nogo-C was only detectable in the Nogo-C sample, providing the evidence of the high efficiency of the immunopurification. Five peptides of the core protein Nogo-C were detected, with a total peptide sequence coverage of 43% (**Figure 3C**), and the illustration of the representative fragment of Nogo-C was shown in **Figure 3D**.

To better characterize the Among the 73 proteins, 71 proteins (97.2%) were of known functions, which could be characterized into five groups according to their molecular functions. Seven proteins are structural molecules of cytoskeleton, including TUBA8, COPA and MYL4. Forty-three proteins are proteins binding with various components of cells, such as DNA,

Table 1. Summary of Nogo-C interacting proteins identified

Accession	Annotation[a]	mW (Da)	Peptides[b]	PLGS Score	pI (pH)	molecular function[c]
structural molecule						
IPI00478908.3	TUBA1C	28545	4	24.9027	5.0944	SCOC; GTP-A
IPI00007752.1	TUBB2C	49799	7	25.3933	4.602	SCOC; GTP-A
IPI00387144.5	TUBA1B	57723	4	10.9827	4.7631	SMA; GTP-A
IPI00791613.1	TUBA8	51951	2	7.4946	4.9852	SCOC; GTP-A
IPI00295857.7	COPA	138257	13	19.4444	7.4464	SMA
IPI00646493.1	COPA	139235	5	7.1371	7.3354	SMA
IPI00386712.1	MYL4	21550	2	15.736	4.7834	SCOM; AF-B
binding						
IPI00011253.3	RPS3	26671	6	27.1605	10.0402	SCOR
IPI00878297.1	RPS2	29984	4	24.9084	8.9835	SCOR; FGF-B
IPI00877699.1	TRIOBP	28939	7	21.4844	5.5144	MGRA-B
IPI00014149.3	TTC35	34811	3	14.1414	6.1335	binding
IPI00029266.1	SNRPE	10796	2	25	9.7804	DR-B; RNA-S
IPI00644224.2	HNRNPU	86806	14	27.551	6.0108	DRP-B
IPI00908896.1	HNRNPH	16838	2	30.1887	4.821	RP-B
IPI00644079.2	HNRNPU	90527	14	1222.6204	5.6479	RP-B
IPI00643152.2	HSP70	77513	8	17.305	8.1035	PA-B
IPI00910482.1	HSP70	61492	10	445.444	5.2773	PA-B
IPI00878876.1	SNRPD3	13282	2	15.8333	9.2411	RP-B
IPI00167147.1	HNRNPU	90235	11	25.3731	6.4883	RP-B
IPI00219037.5	H2AFX	15135	2	11.1888	11.1559	DP-B
IPI00642249.1	AMOT	68350	4	8.7102	8.016	P-B
IPI00028888.1	HNRNPD	38410	3	9.5775	7.8979	DP-B; TF
IPI00479191.2	HNRNPH	51197	5	32.4153	6.3431	DRP-B
IPI00013877.2	HNRNPH	36903	3	11.2717	6.3999	RP-B
IPI00479217.1	HNRNPU	88924	14	25.6824	5.4659	DRPA-B
IPI00217030.10	RPS4X	29579	5	28.1369	10.5861	D-B
IPI00916188.1	NCL	32427	4	21.8855	5.0956	RP-B
IPI00604620.3	NCL	76568	4	139.2712	4.4004	RP-B
IPI00402185.4	SYNCRIP	46299	3	9.5122	9.1055	PS; RP-B
IPI00641719.1	SURF4	21113	5	19.3548	6.0936	P-B
IPI00399142.5	SURF4	21115	2	21.8085	8.7072	P-B
IPI00023673.1	LGALS3BP	65289	3	11.453	4.9438	P-B
IPI00887555.1	LGALS3BP	61605	4	86.0234	5.1229	P-B
IPI00889009.1	RPL23A	22681	3	11.1111	10.5355	SCOR; DRP-B
IPI00455428.3	RPS2	29745	4	13.8182	10.3555	SCOR; FGF-B
IPI00888294.1	RPS2	25528	4	18.4549	10.2367	SCOR; FGF-B
IPI00187140.1	RPS26	12993	2	18.2609	10.9547	SCOR; RP-B
IPI00886830.1	RPS16	18223	2	10.9756	9.4964	SCOR; RP-B
IPI00397609.2	RPS18	17627	5	28.9474	10.7721	SCOR; R-B
IPI00909890.1	FUS	44785	8	24.9417	9.1479	DRPI-B
IPI00260715.5	FUS	53344	7	675.9695	9.559	DRPI-B
IPI00045801.3	FIZ1	51960	2	5.0403	8.0577	DPI-B
IPI00397701.3	RPS16	16401	4	26.7123	10.3768	RP-B
IPI00456429.3	UBA52	14718	3	27.3438	10.2647	P-B

IPI00789951.2	CALML4	21459	3	15.8974	6.7083	Ca^{2+}-B
IPI00478437.3	CALML4	21869	2	14.7959	7.4013	Ca^{2+}-B
IPI00014456.4	STRN	86078	4	6.5385	4.9459	Ca^{2+}-B; CA
IPI00219806.7	S100A7	11463	2	21.7822	6.3404	ZI/Ca^{2+}-B
IPI00845339.1	HSP70	69995	21	34.4774	5.3154	DPA-B; UPL-B
IPI00005667.4	N4BP1	100345	6	11.8304	5.0488	MI-B
signal transducer						
IPI00873380.1	Nogo C	22238	25	43.2161	9.5266	ST; P-B
IPI00021766.5	RTN4	129851	22	7.047	4.2241	ST; P-B
IPI00298289.1	RTN4	40292	10	26.2735	4.4905	ST; P-B
IPI00219207.1	RTN4	22381	27	34.6734	9.6482	ST; P-B
IPI00477663.1	RTN4	106294	21	6.9792	4.2167	ST; P-B
IPI00894099.1	RTN4	22791	9	28.5714	9.0452	ST; P-B
IPI00478442.3	RTN4	42247	7	18.3673	4.4485	ST; P-B
IPI00894213.1	RTN4	108382	3	5.2738	4.3154	ST; P-B
IPI00220880.1	RGS20	31465	4	24.9084	5.04	ST; P-B
IPI00303797.3	B-RAF	84383	2	179.4723	7.2643	MAPKKK
IPI00020898.1	RPS6KA3	83683	5	12.8378	6.4204	MAPKKK
transcription regulator activity						
IPI00641665.1	ILF2	12374	4	63.4783	4.8984	TF
IPI00011274.3	HNRPDL	46409	5	14.5238	9.8221	TF; DRP-B
IPI00798127.1	UBC	76981	3	4.9635	7.7573	T; COR
IPI00798155.4	UBC	12229	4	29.2453	10.5756	T; COR
IPI00556173.1	ILF3	76454	5	9.3484	7.853	TR; I-B
IPI00298788.4	ILF3	95279	5	9.9553	8.9555	TF
transporter						
IPI00797148.1	HNRNPA1	29368	7	33.3333	9.4607	RNA TT
IPI00879501.2	HNRNPA1	34204	5	16.875	9.2814	RNA TT
IPI00644968.1	HNRNPA1	34202	6	23.75	9.4684	RNA TT
IPI00176692.7	HNRNPA1	32142	5	495.4168	9.1154	RNA TT
IPI00478539.2	HNRNPA1	32360	5	21.5947	9.1631	RNA TT
unknown function						
IPI00902571.1	TNRC18	169808	5	7.8076	7.1545	unknown
IPI00186448.7	TNRC18	64571	3	10.2564	10.2389	unknown

Notes: [a]The gene name encoding for each protein identified; [b]Number of unique peptides found for each protein identified; [c]SCOC, structural constituent of cytoskeleton; GTP-A, GTP activation; SMA, structural molecule activity; SCOM, structural constituent of muscle; SCOR, structural constituent of ribosome; RNA-B, RNA binding; FGF-B, FGF binding; MGRA-B, myosin/GTP-Rho/actin binding; DRP-B, DNA/RNA/protein binding; D-B, DNA binding; DR-B, DNA/RNA binding; RNA-S, RNA splicing; RP-B, RNA/protein binding; PA-B, protein/ATP binding; DP-B, DNA/protein binding; P-B, protein binding; TF, transcription factor; DRPA-B, protein/RNA/DNA/ATP binding; PS, protein stabilization; DRPI-B, DNA/RNA/protein/ion binding; DPI-B, protein kinase/DNA/ion binding; Ca^{2+}-B, Ca^{2+} binding; CA, catalytic activity; ZI/Ca^{2+}-B, zinc ion/Ca^{2+} binding; MI-B, metal ion binding; ST, signal transducer; MAPKKK, MAP kinase kinase kinase activity; COR, constituents of ribosome; TR, transcription repressor; I-B, ion binding; DPA-B, DNA/Protein/ATP binding; UPL-B, ubiquitin protein ligase binding; RNA TT, RNA transmembrane transporter; R-B, RNA binding; AF-B, actin filament binding.

RNA, Protein, ion, Ca^{2+} or ATP, including TRIOBP, AMOT, SNRPE, SYNCRIP, SURF4, LGALS3BP, CALML4, STRN, S100A7, N4BP1 and HSPA1B. Ten proteins are signal transducer, including RTN4 family proteins, B-RAF and RGS20. Six proteins are transcription-related proteins, including RPS6KA3, UBC and ILF3. Five HNRNPA1 proteins are detected functioning as RNA transporter. The rest two TNRC18 proteins are of still unknown functions to our knowledge, and need more investigation. The highly diverse of interaction proteins and their multi functions indicated the complication of Nogo-C function. Other RTN4 family members were detected to

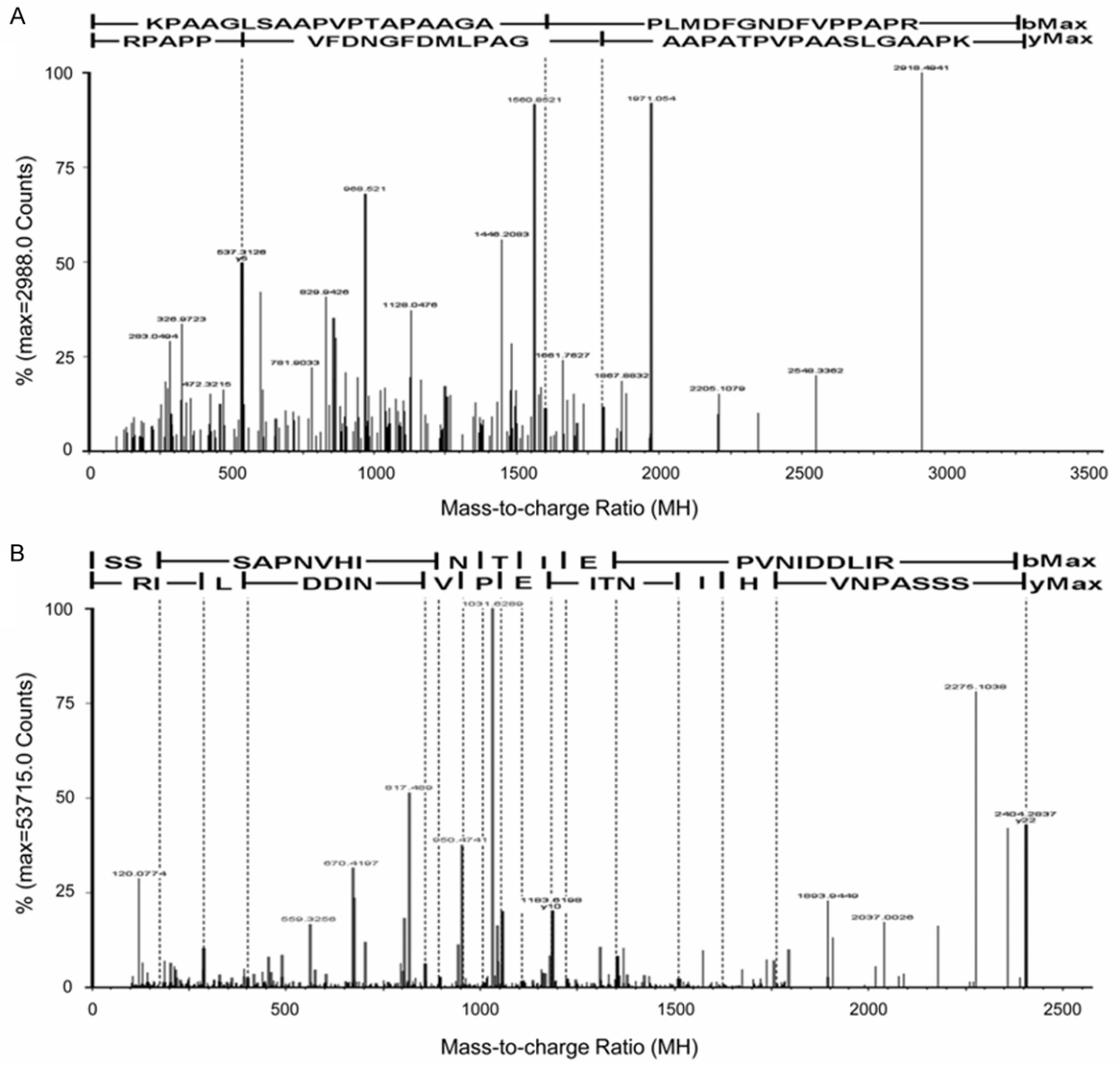

Figure 4. Peptides of selected proteins identified by MS/MS spectrum. A: The MS/MS sequencing of the specific peptide of Nogo-B: KPAAGLSAAPVPTAPAAGAPLMDFGNDFVPPAPR. B: The MS/MS sequencing of the specific peptide of B-RAF: SSSAPNVHINTIEPVNIDDLIR. Reversed database searching were performed to optimize the specificity of the data, and the results were shown under the sequence of each peptide.

bind with Nogo-C, demonstrating the previously reported interaction between Nogo-A, -B and -C through their hydrophobic reticulon domain.

Nogo-B and B-Raf interacted with Nogo-C

To confirm the interaction between Nogo-C and proteins identified by mass spectrometry, Nogo-B and B-Raf were chosen for validations. Their unique MS/MS sequencing peptides were shown in **Figure 4**.

Co-IP experiments were first performed for the verification of the possible interactions. The plasmids of the proteins to be validated were transfected into SMMC-7721 cells together with the Nogo-C plasmid. Western blots were performed to trace the proteins and as shown in **Figure 5A** and **5B**, Myc-Nogo-C was detectable at approximately 25 KD after being immunoprecipitated with anti-HA monoclonal antibody. In the 'reciprocal' IP experiment, the protein of Myc-B-Raf was also detectable at approximately 85 KD with anti-Myc antibody.

Then the subcellular localization of the protein complexes were observed in SMMC-7721 cells using confocal. The intracellular localization of

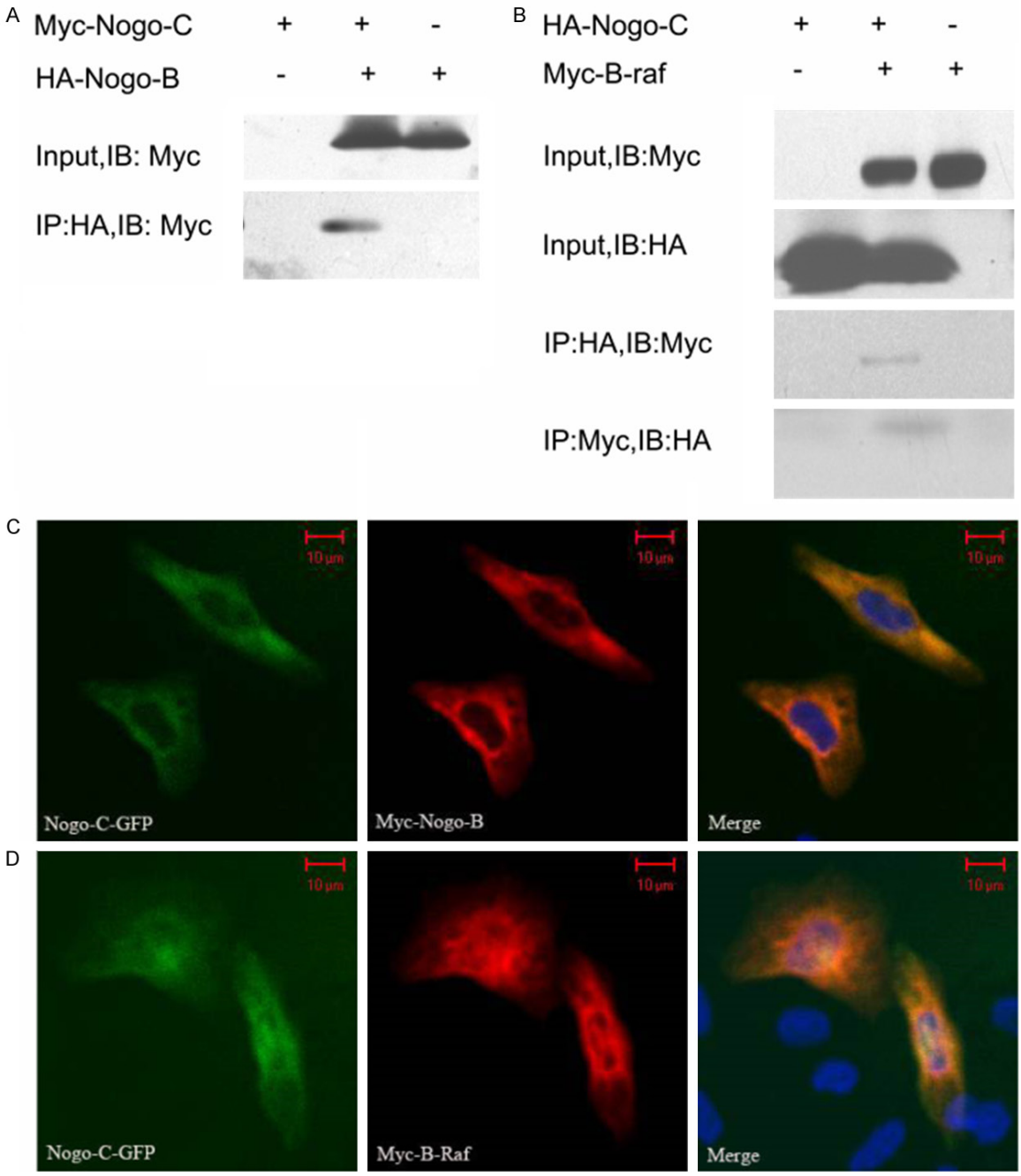

Figure 5. Verification of identified protein binding with Nogo-C. Co-immunoprecipitation and intracellular co-localization between identified proteins and Nogo-C were performed. A: Myc-Nogo-C and HA-Nogo-B. B: HA-Nogo-C and Myc-B-Raf. Both forward and reciprocal immunoprecipitations were performed using anti-HA or anti-Myc monoclonal antibody. C: Co-localization of exogenous Myc-Nogo-B and Nogo-C-GFP. D: Co-localization of exogenous Myc-B-Raf and Nogo-C-GFP. primary anti-Myc monoclonal antibody and Alexa Fluor 488-congulated secondary antibody were used. SMMC-7721 cells were observed by confocal laser scanning microscope. Bars represent 10 μm.

Nogo-C-Nogo-B complex co-localized in cytoplasm (**Figure 5C**) while Nogo-C-B-Raf complex was in both cytoplasm and nucleus (**Figure 5D**), which might be affected by the dual localization of B-raf.

Discussion

Nogo-C is a member of Nogo family with no well-known functions. In this study, we identified Nogo-C as a tumor suppressor gene in

HCC, and B-raf as a novel interacting protein of Nogo-C. This study is the first high-throughput functional proteomic analysis on Nogo-C. The validity of our data was supported by two evidences. First, the high peptide sequence coverage of Nogo-C in test samples convinces the specificity and efficiency of the immunopurification; Second, the identification of other members of Nogo family, coincident with the previously reported interaction among Nogo-A, -B, -C [23]. The remaining proteins are supposed to form complex with Nogo-C in either direct or indirect way. Function of Nogo-C could be analyzed according to these protein complexes.

B-Raf is one of the key moleculars consisting the mitogen-activated protein kinase (MAPK) pathway, and involved in the control of cell growth, proliferation, and migration in majority of the cancers [24]. Antagonism of B-raf using sorafenib is demonstrated to be effective in HCC [25]. For the first time, we demonstrated the interaction between Nogo-C and B-Raf and suggested the relationship between Nogo-C and RAF/MAPK pathway. It is possible for Nogo-C to modulate the kinase activity by altering its phosphorylation and tethering signaling components to a specific area of the cell like the previously reported interacting proteins; or to function as a physiological substrate of the kinase, similarly with its homolog Nogo-B [26].

Coatomer-alpha subunit (COPA) and Surf4 are ER-located proteins with dilysine motif identified in our results. Abundance of peptides identified and the overlapping localization with Nogo-C intensively suggested the possibility of interactions. Functioning as cargo receptors, both COPA and Surf4 not only mediate proteins sorting in anterograde and retrograde cellular transportation in the secretory pathway, but also stabilize the cellular membrane architecture in an oligomeric state [27-29]. Reticulons, including Nogo-A, have been reported to be a key component to structurally shape ER tubules [30, 31]. Thus, it is highly possible for Nogo-C to function with the same region, forming complexes with the proteins identified, in either protein trafficking or ER tubule formation.

Disclosure of conflict of interest

None.

Address correspondence to: Dr. De-Chun Geng, Department of Orthopaedic Surgery, The First Affiliated Hospital of Soochow University, 188 Shizi Road, Suzhou, Jiangsu 215006, China. Tel: +86 512 67780999; Fax: +86 512 67780999; E-mail: szgengdc@163.com; Dr. Long Yu, State Key Laboratory of Genetic Engineering, Fudan University, 220 Handan Road, Shanghai, 200433, China. Tel: +86 21 65643713; Fax: +86 21 65643250; E-mail: yulong201@aliyun.com

References

[1] BI Anding YL, Yang J, Zhang M, Zhou Y and Zhao SY. Cloning and expression analysis of human reticulon 4c cDNA. Chinese Science Bulletin 2000; 45: 1862-1869.

[2] Yang YS and Strittmatter SM. The reticulons: a family of proteins with diverse functions. Genome Biol 2007; 8: 234.

[3] Bullard TA, Protack TL, Aguilar F, Bagwe S, Massey HT and Blaxall BC. Identification of Nogo as a novel indicator of heart failure. Physiol Genomics 2008; 32: 182-189.

[4] Paszkowiak JJ, Maloney SP, Kudo FA, Muto A, Teso D, Rutland RC, Westvik TS, Pimiento JM, Tellides G, Sessa WC and Dardik A. Evidence supporting changes in Nogo-B levels as a marker of neointimal expansion but not adaptive arterial remodeling. Vascul Pharmacol 2007; 46: 293-301.

[5] Rodriguez-Feo JA, Hellings WE, Verhoeven BA, Moll FL, de Kleijn DP, Prendergast J, Gao Y, van der Graaf Y, Tellides G, Sessa WC and Pasterkamp G. Low levels of Nogo-B in human carotid atherosclerotic plaques are associated with an atheromatous phenotype, restenosis, and stenosis severity. Arterioscler Thromb Vasc Biol 2007; 27: 1354-1360.

[6] Yu J, Fernandez-Hernando C, Suarez Y, Schleicher M, Hao Z, Wright PL, DiLorenzo A, Kyriakides TR and Sessa WC. Reticulon 4B (Nogo-B) is necessary for macrophage infiltration and tissue repair. Proc Natl Acad Sci U S A 2009; 106: 17511-17516.

[7] Oertle T and Schwab ME. Nogo and its paRTNers. Trends Cell Biol 2003; 13: 187-194.

[8] Zhang D, Utsumi T, Huang HC, Gao L, Sangwung P, Chung C, Shibao K, Okamoto K, Yamaguchi K, Groszmann RJ, Jozsef L, Hao Z, Sessa WC and Iwakiri Y. Reticulon 4B (Nogo-B) is a novel regulator of hepatic fibrosis. Hepatology 2011; 53: 1306-15.

[9] Chen Y, Tang X, Cao X, Chen H and Zhang X. Human Nogo-C overexpression induces SMMC-7721 cell apoptosis via a mechanism that involves JNK-c-Jun pathway. Biochem Biophys Res Commun 2006; 348: 923-928.

[10] Kim JE, Bonilla IE, Qiu D and Strittmatter SM. Nogo-C is sufficient to delay nerve regeneration. Mol Cell Neurosci 2003; 23: 451-459.

[11] Magnusson C, Libelius R and Tagerud S. Nogo (Reticulon 4) expression in innervated and denervated mouse skeletal muscle. Mol Cell Neurosci 2003; 22: 298-307.
[12] Jung TY, Jung S, Lee KH, Cao VT, Jin SG, Moon KS, Kim IY, Kang SS, Kim HS and Lee MC. Nogo-A expression in oligodendroglial tumors. Neuropathology 2011; 31: 11-9.
[13] Marucci G, Di Oto E, Farnedi A, Panzacchi R, Ligorio C and Foschini MP. Nogo-A: a useful marker for the diagnosis of oligodendroglioma and for identifying 1p19q codeletion. Hum Pathol 2012; 43: 374-80.
[14] Xiong NX, Zhao HY, Zhang FC and He ZQ. Negative correlation of Nogo-A with the malignancy of oligodendroglial tumor. Neurosci Bull 2007; 23: 41-45.
[15] Xiao W, Zhou S, Xu H, Li H, He G, Liu Y and Qi Y. Nogo-B promotes the epithelial-mesenchymal transition in SMMC-7721 cervical cancer cells via Fibulin-5. Oncol Rep 2013; 29: 109-16.
[16] Uetz P, Giot L, Cagney G, Mansfield TA, Judson RS, Knight JR, Lockshon D, Narayan V, Srinivasan M, Pochart P, Qureshi-Emili A, Li Y, Godwin B, Conover D, Kalbfleisch T, Vijayadamodar G, Yang M, Johnston M, Fields S and Rothberg JM. A comprehensive analysis of protein-protein interactions in Saccharomyces cerevisiae. Nature 2000; 403: 623-627.
[17] Fournier AE, GrandPre T and Strittmatter SM. Identification of a receptor mediating Nogo-66 inhibition of axonal regeneration. Nature 2001; 409: 341-346.
[18] Hu WH, Hausmann ON, Yan MS, Walters WM, Wong PK and Bethea JR. Identification and characterization of a novel Nogo-interacting mitochondrial protein (NIMP). J Neurochem 2002; 81: 36-45.
[19] Tagami S, Eguchi Y, Kinoshita M, Takeda M and Tsujimoto Y. A novel protein, RTN-XS, interacts with both Bcl-XL and Bcl-2 on endoplasmic reticulum and reduces their anti-apoptotic activity. Oncogene 2000; 19: 5736-5746.
[20] Kersey PJ, Duarte J, Williams A, Karavidopoulou Y, Birney E and Apweiler R. The International Protein Index: an integrated database for proteomics experiments. Proteomics 2004; 4: 1985-1988.
[21] Jiang M, Gao Y, Yang T, Zhu X and Chen J. Cyclin Y, a novel membrane-associated cyclin, interacts with PFTK1. FEBS Lett 2009; 583: 2171-2178.
[22] Gotz S, Garcia-Gomez JM, Terol J, Williams TD, Nagaraj SH, Nueda MJ, Robles M, Talon M, Dopazo J and Conesa A. High-throughput functional annotation and data mining with the Blast2GO suite. Nucleic Acids Res 2008; 36: 3420-3435.
[23] Dodd DA, Niederoest B, Bloechlinger S, Dupuis L, Loeffler JP and Schwab ME. Nogo-A, -B, and -C are found on the cell surface and interact together in many different cell types. J Biol Chem 2005; 280: 12494-12502.
[24] Colombino M, Sperlongano P, Izzo F, Tatangelo F, Botti G, Lombardi A, Accardo M, Tarantino L, Sordelli I, Agresti M, Abbruzzese A, Caraglia M and Palmieri G. BRAF and PIK3CA genes are somatically mutated in hepatocellular carcinoma among patients from South Italy. Cell Death Dis 2012; 3: e259.
[25] Llovet JM, Ricci S, Mazzaferro V, Hilgard P, Gane E, Blanc JF, de Oliveira AC, Santoro A, Raoul JL, Forner A, Schwartz M, Porta C, Zeuzem S, Bolondi L, Greten TF, Galle PR, Seitz JF, Borbath I, Haussinger D, Giannaris T, Shan M, Moscovici M, Voliotis D and Bruix J. Sorafenib in advanced hepatocellular carcinoma. N Engl J Med 2008; 359: 378-390.
[26] Rousseau S, Peggie M, Campbell DG, Nebreda AR and Cohen P. Nogo-B is a new physiological substrate for MAPKAP-K2. Biochem J 2005; 391: 433-440.
[27] Nyfeler B, Reiterer V, Wendeler MW, Stefan E, Zhang B, Michnick SW and Hauri HP. Identification of ERGIC-53 as an intracellular transport receptor of alpha1-antitrypsin. J Cell Biol 2008; 180: 705-712.
[28] Nyfeler B, Zhang B, Ginsburg D, Kaufman RJ and Hauri HP. Cargo selectivity of the ERGIC-53/MCFD2 transport receptor complex. Traffic 2006; 7: 1473-1481.
[29] Nyfeler B, Michnick SW and Hauri HP. Capturing protein interactions in the secretory pathway of living cells. Proc Natl Acad Sci U S A 2005; 102: 6350-6355.
[30] Shibata Y, Voss C, Rist JM, Hu J, Rapoport TA, Prinz WA and Voeltz GK. The reticulon and DP1/Yop1p proteins form immobile oligomers in the tubular endoplasmic reticulum. J Biol Chem 2008; 283: 18892-18904.
[31] Voeltz GK, Prinz WA, Shibata Y, Rist JM and Rapoport TA. A class of membrane proteins shaping the tubular endoplasmic reticulum. Cell 2006; 124: 573-586.